

## GENE THERAPY

# Intein-mediated protein trans-splicing expands adeno-associated virus transfer capacity in the retina

Patrizia Tornabene<sup>1\*</sup>, Ivana Trapani<sup>1,2\*</sup>, Renato Minopoli<sup>1</sup>, Miriam Centrulo<sup>1</sup>, Mariangela Lupo<sup>1</sup>, Sonia de Simone<sup>1</sup>, Paola Tiberi<sup>1</sup>, Fabio Dell'Aquila<sup>1</sup>, Elena Marrocco<sup>1</sup>, Carolina Iodice<sup>1</sup>, Antonella Iuliano<sup>1</sup>, Carlo Gesualdo<sup>3</sup>, Settimio Rossi<sup>3</sup>, Laura Giaquinto<sup>1</sup>, Silvia Albert<sup>4</sup>, Carel B. Hoyng<sup>5</sup>, Elena Polishchuk<sup>1</sup>, Frans P. M. Cremers<sup>5</sup>, Enrico M. Surace<sup>1,2</sup>, Francesca Simonelli<sup>3</sup>, Maria A. De Matteis<sup>1,6</sup>, Roman Polishchuk<sup>1</sup>, Alberto Auricchio<sup>1,7†</sup>

Copyright © 2019  
The Authors, some  
rights reserved;  
exclusive licensee  
American Association  
for the Advancement  
of Science. No claim  
to original U.S.  
Government Works

Retinal gene therapy with adeno-associated viral (AAV) vectors holds promises for treating inherited and noninherited diseases of the eye. Although clinical data suggest that retinal gene therapy is safe and effective, delivery of large genes is hindered by the limited AAV cargo capacity. Protein trans-splicing mediated by split inteins is used by single-cell organisms to reconstitute proteins. Here, we show that delivery of multiple AAV vectors each encoding one of the fragments of target proteins flanked by short split inteins results in protein trans-splicing and full-length protein reconstitution in the retina of mice and pigs and in human retinal organoids. The reconstitution of large therapeutic proteins using this approach improved the phenotype of two mouse models of inherited retinal diseases. Our data support the use of split intein-mediated protein trans-splicing in combination with AAV subretinal delivery for gene therapy of inherited blindness due to mutations in large genes.

## INTRODUCTION

The first adeno-associated viral (AAV) vector-based gene therapy product for an inherited form of blindness was approved in December 2017 (1). In addition, a number of other AAV-based products are currently under clinical development for gene therapy of rare and common forms of blindness (2). Although it is now well established that AAV represents, to date, the most efficient gene therapy vehicle for the retina (2, 3), its limited cargo capacity (2) has hampered its use for conditions that require delivery of DNA sequences that exceed 5 kb in size including not only the transgene but also the cis regulatory elements that are necessary for its expression. We and others have shown that this limitation can be overcome by using either dual (up to 9 kb) (4–6) or triple (up to 14 kb) (7) AAV vectors, each containing fragments of the coding sequence (CDS) of the large transgene expression cassette. Dual and triple AAV vectors exploit concatemerization and recombination of AAV genomes to reconstitute the full-length genomes in cells coinfecting by multiple AAV vectors. However, the efficiency of transgene expression achieved with either dual or triple AAV vectors in photoreceptors, which are the main therapeutic targets for most inherited retinal diseases, is lower than that achieved with single AAV vectors (4, 7, 8). This might be due to the various limiting steps required for efficient transduction including proper DNA concatemer formation, stability of the heterogeneous mRNA, and splicing efficiency across the junctions of the vectors.

Inteins are genetic elements present in unicellular organisms, transcribed and translated as an internal polypeptide segment within a host protein (9, 10). Posttranslationally, they mediate their self-excision from the precursor protein, without leaving amino acid modifications in the final protein product. Protein splicing mediated by inteins does not require energy supply, exogenous host-specific proteases, or cofactors (9, 10). Intein activity is context dependent, with certain peptide sequences surrounding their ligation junction (called N- and C-exteins) that are required for efficient trans-splicing to occur, of which the most important is an amino acid containing a thiol or hydroxyl group (Cys, Ser, or Thr) as first residue in the C-extein (11). Split inteins are a subset of inteins that are expressed as two separate polypeptides at the ends of two host proteins and catalyze their trans-splicing, resulting in the generation of a single larger polypeptide (12). Inteins, including split inteins, are widely used in biotechnological applications that include protein purification and labeling steps (12, 13), as well as the reconstitution of the widely used clustered regularly interspaced short palindromic repeats (CRISPR)–Cas9 genome editing nuclease (14, 15).

In this study, we took advantage of the intrinsic ability of split inteins to mediate protein trans-splicing to reconstitute large full-length proteins after their fragmentation into either two or three split intein-flanked polypeptides whose sequences fit into single AAV vectors. We tested the efficiency of AAV intein in the retina by delivering the enhanced green fluorescent protein (*EGFP*) gene and the large ATP (adenosine 5'-triphosphate)-binding cassette subfamily A member 4 (*ABCA4*) and centrosomal protein 290 (*CEP290*) genes, which are defective in two common forms of severe inherited retinal diseases: Stargardt disease (STGD1) and Leber congenital amaurosis type 10 (LCA10), respectively. We compared the efficiency of transgene expression achieved with AAV intein to that of either single or dual AAV vectors in vitro and in vivo and used mouse and pig retina and human retinal organoids. We also investigated the efficacy of AAV intein in improving the retinal phenotypes in mouse models of STGD1 and LCA10.

<sup>1</sup>Telethon Institute of Genetics and Medicine (TIGEM), 80078 Pozzuoli, Italy. <sup>2</sup>Medical Genetics, Department of Translational Medicine, Federico II University, 80131 Naples, Italy. <sup>3</sup>Eye Clinic, Multidisciplinary Department of Medical, Surgical and Dental Sciences, University of Campania L. Vanvitelli, 80131 Naples, Italy. <sup>4</sup>Department of Human Genetics and Donders Institute for Brain, Cognition and Behaviour, Radboud University Medical Center, 6525 Nijmegen, Netherlands. <sup>5</sup>Department of Ophthalmology and Donders Institute for Brain, Cognition and Behaviour, Radboud University Medical Center, 6525 Nijmegen, Netherlands. <sup>6</sup>Department of Molecular Medicine and Medical Biotechnology, Federico II University, 80131 Naples, Italy. <sup>7</sup>Department of Advanced Biomedicine, Federico II University, 80131 Naples, Italy.

\*These authors contributed equally to this work.

†Corresponding author. Email: auricchio@tigem.it

**RESULTS****AAV-EGFP intein vectors reconstitute full-length proteins in vitro**

To test the efficiency of intein-mediated protein trans-splicing in the retina, we generated two AAV vectors each encoding either the N- or the C-terminal half of the reporter EGFP protein fused to the N- and C-terminal halves of the DnaE split intein from *Nostoc punctiforme* (Fig. 1A) (16, 17), respectively. Each AAV vector included appropriate regulatory elements (promoter and a polyadenylation signal) and a triple flag tag (3xflag) to allow detection of both halves and the full-length reconstituted EGFP protein (Fig. 1A).

AAV-EGFP intein plasmids were used to transfect HEK293 cells and evaluate the production of single N- and C-terminal halves as well as of the full-length EGFP protein. EGFP fluorescence was detected only in cells transfected either with a single AAV plasmid that encodes full-length EGFP or with the combination of AAV-EGFP intein plasmids but not with the single N- and C-terminal AAV-EGFP intein plasmids (fig. S1). Trans-spliced EGFP protein of the expected size (~28 kDa) along with DnaE intein (~17 kDa) spliced out from the mature protein were detected by WB analysis of HEK293 cell lysates after cotransfection only of both AAV-EGFP intein plasmids (Fig. 1B). Quantification of EGFP bands' intensity from AAV intein plasmids and from a single AAV plasmid is shown in fig. S2. To define the accuracy of protein reconstitution, we immunopurified EGFP from HEK293 cells transfected with the AAV-EGFP intein plasmids and performed liquid chromatography–mass spectrometry (LC-MS) analysis to define its protein sequence. The 3532 peptides obtained from proteolytic digestion of this sample, 7 of which included the splitting point (Table 1), covered the whole protein and confirmed that the amino acidic sequence of EGFP reconstituted by AAV intein plasmids precisely corresponds to that of wild-type EGFP.

**AAV-EGFP intein vectors are more efficient than dual AAV vectors in vitro**

To confirm EGFP protein reconstitution from AAV intein vectors, we infected HEK293 cells with either AAV2/2-EGFP intein or with single and dual AAV vectors that included the same expression cassette under the control of the ubiquitous CMV promoter [multiplicity of infection (moi),  $5 \times 10^4$  genome copies (GC) per cell of each vector, which means a similar dose between the three systems assuming that dual vectors undergo complete DNA or protein recombination]. Seventy-two hours after infection, cell lysates were harvested and EGFP expression was evaluated by both Western blot (WB) (Fig. 1C) and enzyme-linked immunosorbent assay (ELISA) to precisely quantify EGFP amounts, which were found to be around half of those achieved with a single AAV and eight times higher than those obtained with dual AAV vectors (fig. S3). Additional quantification of the intensity of full-length EGFP relative to that of excised intein is shown in fig. S4.

**Subretinal administration of AAV-EGFP intein vectors results in efficient full-length protein reconstitution in both mouse and pig retina**

To investigate whether AAV intein-mediated protein trans-splicing reconstitutes full-length protein expression in the retina, we injected subretinally 4-week-old C57BL/6J mice with AAV2/8-CMV-EGFP intein vectors (dose of each vector per eye,  $5.8 \times 10^9$  GC). Eyes were harvested 1 month later and analyzed by microscopy analysis. EGFP fluorescence was detected in all eyes in the retinal pigment epithelium (RPE) and in photoreceptors (Fig. 1D and fig. S5). To compare transgene expression from AAV intein to that of single and

dual AAV in photoreceptors, we injected subretinally in 4-week-old C57BL/6J mice AAV2/8 vectors (dose of each vector per eye,  $5 \times 10^9$  GC) that encode EGFP under the control of the photoreceptor-specific human guanine nucleotide-binding protein (G protein)-coupled receptor kinase 1 (GRK1) promoter. Eyes were harvested 1 month after injection, and EGFP fluorescence from photoreceptor cells (as the photoreceptor-specific GRK1 was used to drive EGFP expression) was detected in eyes injected with all sets of vectors (Fig. 1E and fig. S6). Precise quantification of EGFP protein amounts by ELISA confirmed that AAV intein reconstituted EGFP protein less efficiently than a single AAV and about three times more than dual AAV (fig. S7). The relative amount of full-length EGFP to excised intein after quantification of WB band intensities is shown in fig. S8.

We then evaluated the efficiency of AAV intein vectors at transducing photoreceptors in the pig retina, which is an excellent pre-clinical model to evaluate viral vector transduction due to its size and architecture (18). Thus, we injected subretinally Large White pigs with single, intein, and dual AAV2/8-GRK1-EGFP vectors (dose of each vector per eye,  $2 \times 10^{11}$  GC, delivered through two adjacent subretinal blebs). Eyes were harvested 1 month after injection, and EGFP protein reconstitution in the photoreceptor cell layer mediated by either single, dual, or AAV intein vectors, as assessed by EGFP spontaneous fluorescence, is shown in Fig. 1F. Precise quantification of EGFP in retinal lysates confirmed that AAV intein vectors reconstitute the protein to quantities that are similar to those achieved with a single AAV and about three times higher than those obtained with dual AAV vectors (fig. S9). The relative amount of full-length EGFP to excised intein after quantification of WB band intensities is shown in fig. S10.


**Full-length EGFP is reconstituted by AAV intein-mediated protein trans-splicing in three-dimensional human retinal organoids**

As an additional preclinical model representative of the human retina, we generated three-dimensional (3D) retinal organoids (19, 20) from human induced pluripotent stem cells (iPSC). Six-month-old organoids (Fig. 2A and fig. S11A) contained cells stained by mature photoreceptor markers (Fig. 2B and fig. S11B) and transduced by AAV2 vectors with a photoreceptor-specific promoter (Fig. 2C and fig. S11C). Light (Fig. 2D and fig. S11D) and electron (Fig. 2, E and F, and fig. S11, E and F) microscopies show the presence of buds of photoreceptor outer segments. Nine-month-old 3D human retinal organoids incubated for 30 days with AAV-GRK1-EGFP intein vectors (dose of each vector per organoid,  $1 \times 10^{12}$  GC) show EGFP fluorescence (Fig. 2G and fig. S11G). The relative amount of full-length EGFP to excised intein after quantification of WB band intensities is shown in fig. S12.

**Identification of optimal ABCA4 and CEP290 splitting points is required for efficient AAV intein-mediated protein trans-splicing**

To test whether protein trans-splicing can be developed as a mechanism to reconstitute large therapeutic proteins, we developed AAV-ABCA4 and AAV-CEP290 intein vectors. ABCA4 and CEP290 were split into either two (AAV I and AAV II) or three (AAV I, AAV II, and AAV III) fragments whose coding sequences were separately cloned in single AAV vectors, fused to the coding sequences of the split inteins' N and C termini (fig. S13). The AAV intein vectors included either the ubiquitous short CMV (shCMV) or the GRK1 promoter.

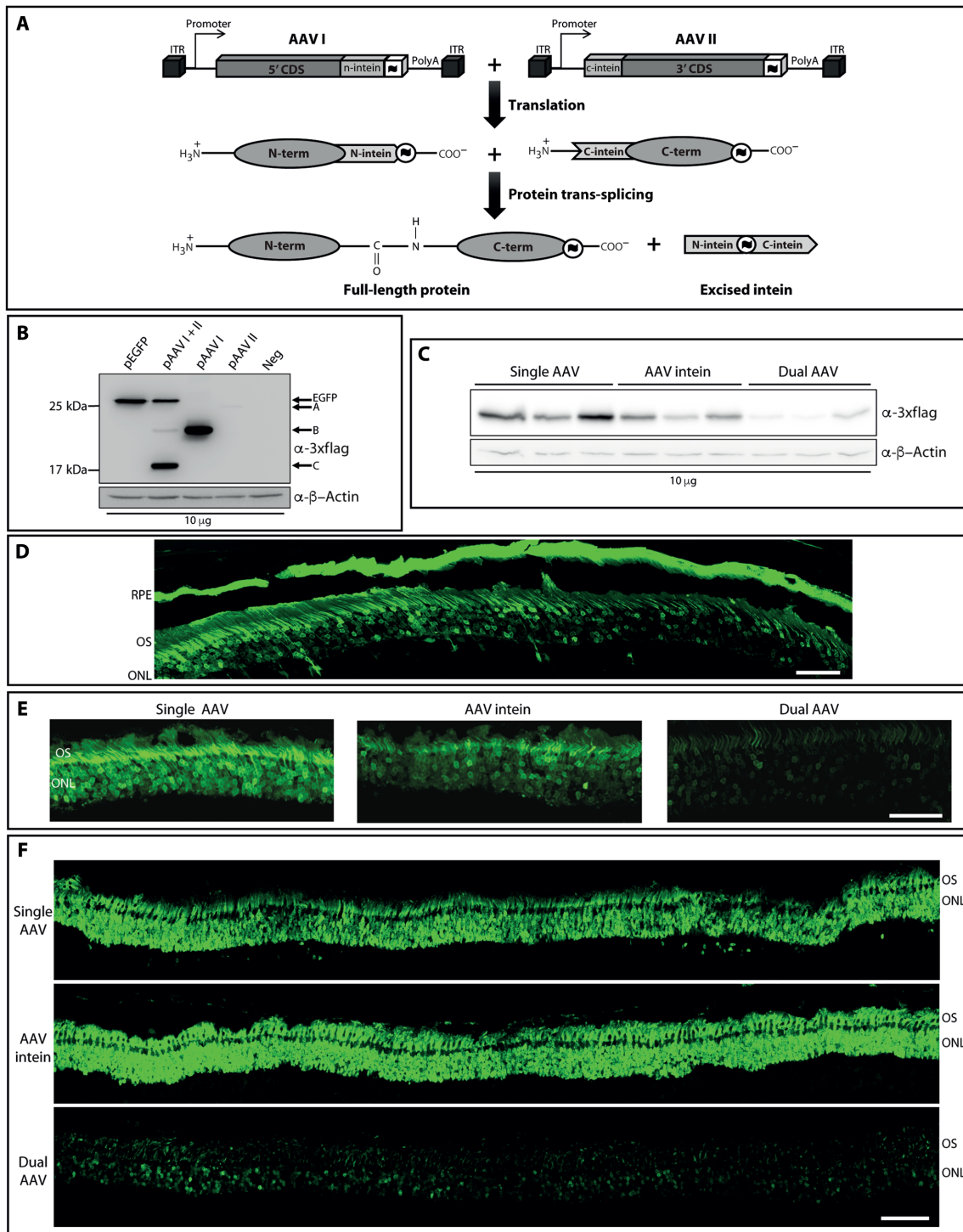


**Fig. 1. AAV intins reconstitute EGFP both in vitro and in mouse and pig retina at levels that are higher than dual AAV and up to those achieved with a single AAV.** (A) Schematic representation of AAV intein-mediated protein trans-splicing. ITR, AAV2 inverted terminal repeats; CDS, coding sequence; , 3xflag tag; PolyA, polyadenylation signal. (B) Western blot (WB) analysis of lysates from human embryonic kidney (HEK) 293 cells transfected with either full-length or AAV intein cytomagalovirus (CMV)-EGFP plasmids. pEGFP, full-length EGFP plasmid; pAAV I + II, AAV-EGFP I + II intein plasmids; pAAV I, single AAV-EGFP I intein plasmid; pAAV II, single AAV-EGFP II intein plasmid; Neg, untransfected cells. The arrows indicate the full-length EGFP protein (EGFP), the N- and C-terminal halves of the EGFP protein (B and A, respectively), and the reconstituted intein excised from the full-length EGFP protein (C). The WB is representative of  $n = 3$  independent experiments. (C) WB analysis of lysates from HEK293 infected with either single, intein, or dual AAV2/2-CMV-EGFP vectors. The WB is representative of  $n = 5$  independent experiments. (D) Retinal cryosection from C57BL/6J mice injected subretinally with AAV2/8-CMV-EGFP intein vectors. Scale bar, 50  $\mu\text{m}$ . RPE, retinal pigment epithelium; OS, outer segments; ONL, outer nuclear layer. The image is representative of  $n = 5$  eyes. (E and F) Retinal cryosections from either C57BL/6J mice (E) or Large White pigs (F) injected subretinally with either single, intein, or dual AAV2/8-GRK1-EGFP vectors. Scale bars, 50  $\mu\text{m}$  (E) and 200  $\mu\text{m}$  (F).

**Table 1. Peptides that include the EGFP splitting point, C<sub>1</sub> cystein-71.**

Peptide sequence	Length
GVQCFSR	7
LPVPWPTLVTTLTLYGVQCFSRY	22
PTLVTTLTLYGVQCFSR	16
TYGVQCFSR	9
YGVQCFSR	8
VQCFSR	6
QCFSR	5

Splitting points for each protein were selected, taking into account both amino acid residue requirements at the junction points for efficient protein trans-splicing (11, 21), as well as preservation of the integrity of critical protein domains, which should favor proper folding and stability of each independent polypeptide and, thus, of the final reconstituted protein. Additional split inteins were also considered. CEP290 sets in which the protein was split into three polypeptides (sets 4 and 5; fig. S13B) were generated to allow the inclusion of the woodchuck hepatitis virus posttranscriptional regulatory element (WPRE) (22) to increase transgene expression. To prevent unwanted trans-splicing between AAV I and AAV III, which could reduce the amount of full-length proteins generated, sets 4 and 5 included two different split inteins at the two splitting junctions, specifically DnaB intein from *Rhodothermus marinus* and either wild-type or a mutated DnaE intein, which we show do not result in detectable EGFP expression when combined and thus do not cross-react (fig. S14).

We compared the ability of each set of AAV intein plasmids to reconstitute ABCA4 and CEP290 after transfection of HEK293 cells. WB analysis of cell lysates 72 hours after transfection showed that full-length ABCA4 and CEP290 proteins of the expected size (~250 and ~290 kDa, respectively) were reconstituted from each set of AAV intein plasmids, although with variable efficiency (Fig. 3, A and B). Sets 1 and 5 tended to be the most efficient for ABCA4 and CEP290 protein reconstitution, respectively, and thus were used in all the subsequent experiments.

To define the accuracy of protein reconstitution, we immunopurified ABCA4 from HEK293 cells transfected with set 1 and performed LC-MS analysis to define its protein sequence. The 3108 peptides obtained from proteolytic digestion of this sample, 22 of which included the splitting point (Table 2), covered the whole protein and confirmed that the amino acidic sequence of ABCA4 reconstituted by AAV intein plasmids precisely corresponds to that of wild-type ABCA4 (fig. S15).

We then assessed the intracellular localization of the protein products of the different intein-containing plasmids, comparing them to the localization of the full-length protein. Full-length ABCA4 is known to localize at the endoplasmic reticulum (ER) when expressed in cultured cell lines (23, 24). We found that the two ABCA4 polypeptides from set 1 show ER colocalization, which is slightly lower for the polypeptide from AAV1 (Fig. 4A). Low localization at the trans-Golgi network was found for all products, in particular for the polypeptide from AAV1 (Fig. 4A). A similar localization was observed in cells cotransfected with both AAV intein plasmids as well as in cells transfected with a plasmid encoding for the full-length ABCA4 protein, thus confirming the predominant localization in the ER of ABCA4 exogenously expressed in cell lines (23, 24).

As for CEP290, it has been reported that the full-length protein shows a mixed distribution pattern with a predominant punctate and a minor fibrillar pattern (25). The dissection of the domains responsible for the subcellular targeting of CEP290 (25) showed that the N-terminal domain (amino acids 1 to 362) targets the protein to vesicular structures thanks to its ability to interact with membranes, whereas a region near the C terminus of CEP290, encompassing much of the protein's myosin tail homology domain, mediates microtubule binding (amino acids 580 to 2479) and, when expressed as a truncated form, has a prominent fibrillar distribution coincident with acetylated tubulin (Ac-tubulin) (25). Consistent with this, products from AAV I and II have a predominant punctate pattern, whereas products from AAV III (encompassing the protein's myosin tail homology domain) show a predominant fibrillar pattern and are the ones that mostly colocalize with Ac-tubulin (Fig. 4B). Thus, the patterns shown by products from AAV I + II, AAV I + III, and AAV II + III are a combination of those shown by the single AAV intein plasmids (Fig. 4B). Cells cotransfected with the three AAV-CEP290 intein plasmids or with the plasmid encoding for the full-length CEP290 protein showed a predominant punctate signal partially aligned along microtubules (Fig. 4B and fig. S16).

We then compared the amount of protein obtained with the best set of AAV-ABCA4 and AAV-CEP290 intein plasmids with those obtained from a single AAV plasmid encoding for the corresponding full-length protein. To this aim, we transfected HEK293 cells with same equimolar amounts of either the single or the AAV intein plasmids, and 72 hours after transfection, cell lysates were analyzed by WB (fig. S17).

### AAV intein vectors mediate expression of large therapeutic proteins in vitro and in the retina

We compared the efficiency of AAV intein-mediated large protein reconstitution with that of dual AAV vectors both in vitro and in the mouse and pig retina. HEK293 cells were infected with either AAV2/2 dual or intein vectors encoding for either ABCA4 or CEP290 (moi,  $5 \times 10^4$  GC per cell of each vector), and cell lysates were analyzed 72 hours later by WB. As shown in Fig. 5A, the intensity of the AAV intein ABCA4 band is higher than that of dual AAV vectors despite the amount of protein lysate loaded was 10-fold lower to avoid saturation. Similarly, as shown in Fig. 5B, CEP290 expression is detected only in cells infected with AAV intein but not with dual AAV vectors. As expected, in addition to full-length proteins, shorter polypeptides derived either from the single AAV intein vectors (in the case of both ABCA4 and CEP290) or from trans-splicing occurring between AAV II and AAV III (in the case of CEP290) were observed (Fig. 5, A and B).

We then injected subretinally 4-week-old wild-type mice with AAV-GRK1-ABCA4 or AAV-GRK1-CEP290 intein versus dual vectors (dose of each ABCA4 vector per eye,  $3.3 \times 10^9$  GC; dose of each CEP290 vector per eye,  $1.1 \times 10^9$  GC). Animals were euthanized 4 to 7 weeks after injection, and protein expression in retinal lysates was evaluated by WB. Full-length proteins were detected in 10 of 11 of the AAV-ABCA4 intein-injected eyes (Fig. 6A and fig. S18) and in 5 of 10 of the AAV-CEP290 intein-injected eyes (Fig. 6B and fig. S19). Conversely, full-length protein expression was evident in 5 of 9 and in 0 of 5 eyes injected with ABCA4 and CEP290 dual AAV vectors, respectively. In addition, we detected polypeptides derived from the single AAV intein vectors (in the case of both ABCA4 and CEP290) and from trans-splicing

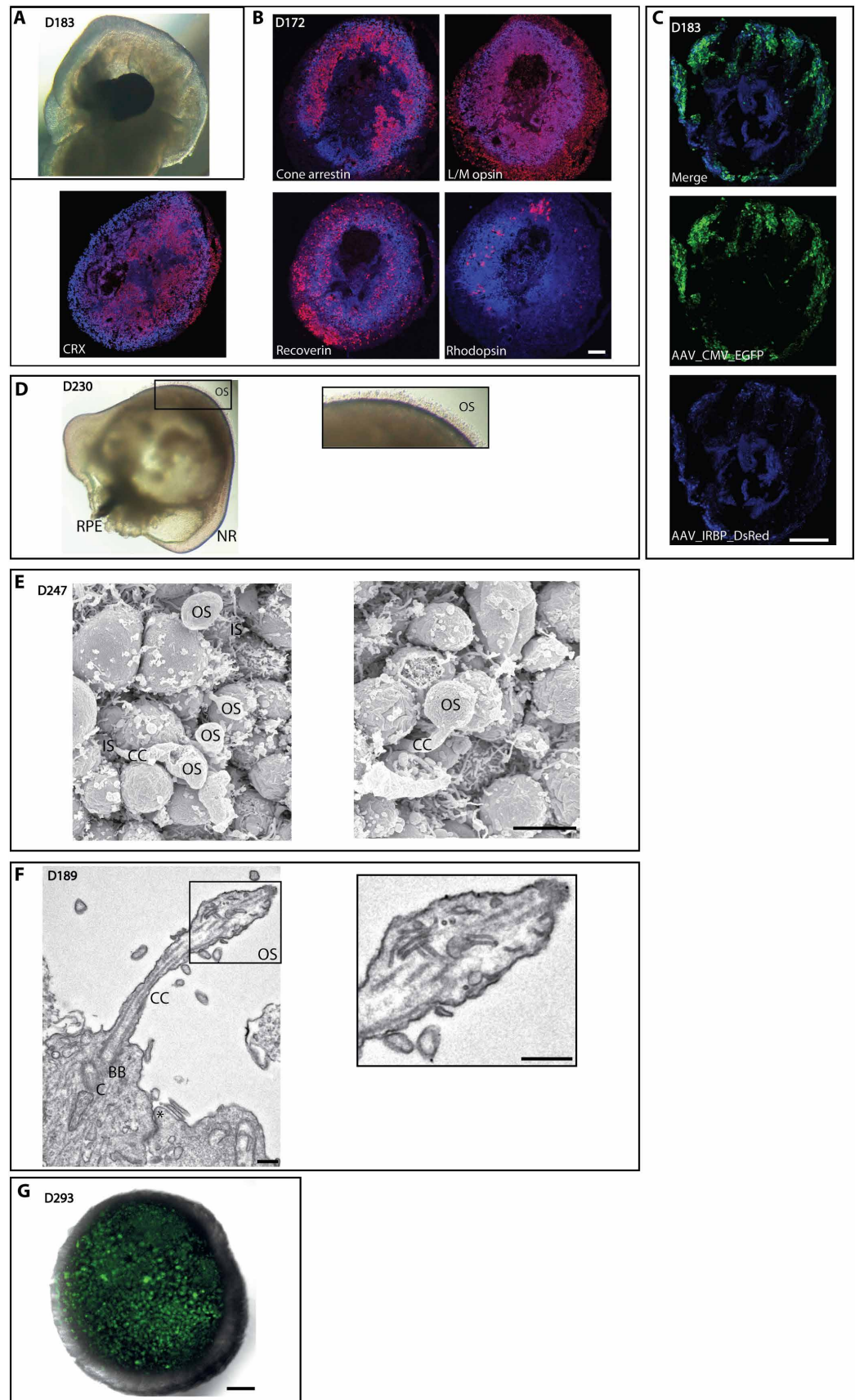
**Fig. 2. Characterization and AAV intein-mediated transduction of human iPSC-derived 3D retinal organoids.**

**(A)** Light microscopy analysis of retinal organoids at 183 days of culture. **(B)** Immunofluorescence analysis with antibodies directed to mature photoreceptor markers. CRX, cone-rod homeobox; L/M opsin, long/medium wavelength opsin. Scale bar, 100  $\mu$ m. **(C)** Fluorescence analysis of retinal organoids infected with both AAV2/2-CMV-EGFP and AAV2/2-DsRed vector under the control of the interphotoreceptor retinoid-binding protein (IRBP) promoter. Scale bar, 100  $\mu$ m. **(D)** OS-like structures were observed, which protrude from the surface of retinal organoids at 230 days of culture. The inset shows the presence of OS-like structures with radial architecture. NR, neural retina. **(E)** Scanning electron microscopy analysis reveals the presence of inner segments (IS), connecting cilia (CC), and OS-like structures. Scale bar, 4  $\mu$ m. **(F)** Electron microscopy analysis reveals the presence of the outer limiting membrane (\*), centriole (C), basal bodies (BB), connecting cilia (CC), and sketches of OS. The inset shows the presence of disorganized membranous discs in the OS. Scale bar, 500 nm. **(G)** Fluorescence analysis of retinal organoids infected with AAV2/2-GRK1-EGFP intein vectors at 293 days of culture. Scale bar, 100  $\mu$ m. The image is representative of  $n = 4$  organoids. (A to G) D, days of culture.

occurring between AAV II and AAV III (in the case of CEP290) (Fig. 6, A and B), as previously observed in vitro.

To investigate the efficiency of protein reconstitution mediated by AAV intein relative to endogenous, we injected subretinally 1- to 4-month-old *Abca4*<sup>-/-</sup> mice with AAV-GRK1-*ABCA4* intein vectors (dose of each *ABCA4* vector per eye,  $5.5 \times 10^9$  GC). One month later, *ABCA4* expression in retinal lysates from unaffected and AAV intein-injected *Abca4*<sup>-/-</sup> mice was analyzed by WB using an antibody that recognizes both murine and human *ABCA4*. The quantification of AAV intein *ABCA4* expression versus endogenous is shown in fig. S20.

To confirm efficient large protein reconstitution in the clinically relevant pig retina, we injected subretinally Large White pigs with either AAV2/8-GRK1-*ABCA4*



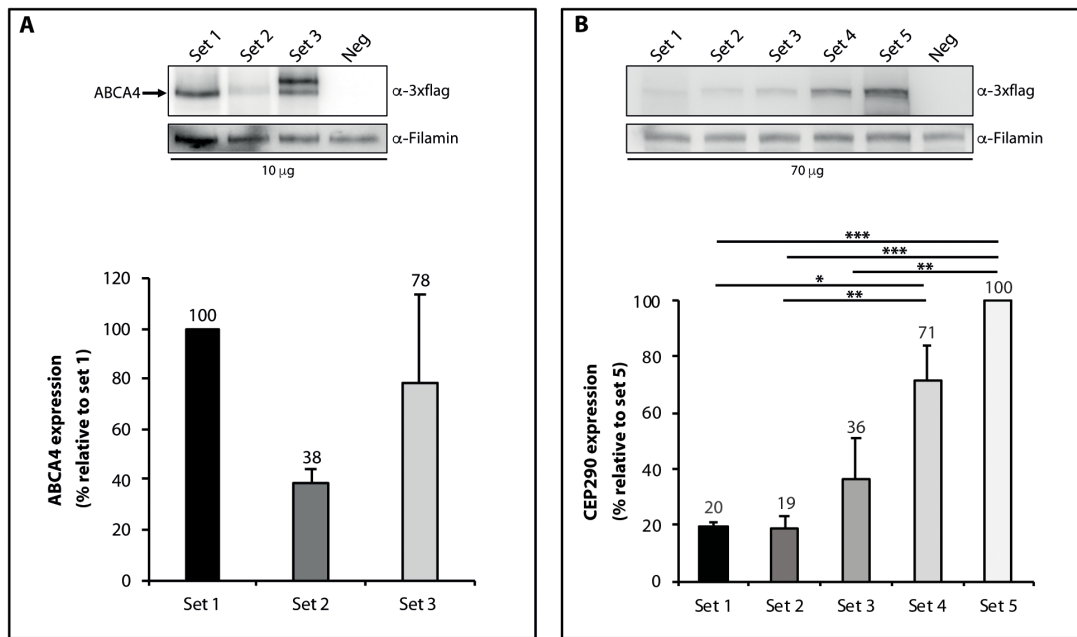


**Fig. 3. Optimization of AAV intein allows proper reconstitution of the large ABCA4 and CEP290 proteins.** WB analysis of lysates from HEK293 transfected with different sets of either AAV-shCMV-ABCA4 or AAV-shCMV-CEP290 intein plasmids. A schematic representation of the various sets used is depicted in fig. S13. The WBs are representative of  $n = 3$  independent experiments. (A) Kruskal-Wallis test  $P$  value was not significant; thus, no post hoc comparison was performed to evaluate statistical differences between groups. (B) Significant differences were assessed using one-way analysis of variance (ANOVA) followed by Tukey multiple pairwise comparison.  $*P < 0.05$ ,  $**P < 0.01$ , and  $***P < 0.001$ . Details on set 1 (A) and set 5 (B) variability can be found in the Statistical analysis section of Materials and Methods.

**Table 2. Peptides that include the ABCA4 splitting point. C**  
cystein-1150.

Peptide sequence	Length
KNCFGT	6
KNCFGTGL (x3)	8
KNCFGTGLY (x2)	9
FLKNCFGTGL	10
KNCFGTGLYLT	11
KNCFGTGLYLT	12
LYCSGTPFLKNC	13
YCSGTPFLKNC	13
KNCFGTGLYLTVR (x7)	14
KNCFGTGLYLTVRKM	16
IAIIAQGRLYCSGTPFLKNC	29
QGRLYCSGTPFLKNC	36
GTPLFLKNC	40

intein or dual vectors (dose of each vector per eye,  $2 \times 10^{11}$  GC, delivered through two adjacent subretinal blebs), and 1 month after injection, we analyzed protein expression by WB. We found that AAV intein reconstitutes full-length ABCA4 protein more efficiently than dual AAV vectors (Fig. 6C).

Last, we infected human retinal organoids from iPSC of either healthy individuals or patients with STGD1 at 121 days of culture [when photoreceptor maturation starts (20)] with AAV2/2-GRK1-ABCA4 intein vectors (dose of each vector per organoid,  $1 \times 10^{12}$

GC). Organoids were lysed between 20 and 40 days after infection and analyzed by WB. ABCA4 of the expected size was detected in all infected organoids ( $n = 3$  and  $n = 4$  from normal control and STGD1 organoids, respectively; Fig. 6D and fig. S21).

**Subretinal administration of AAV intein vectors improves the retinal phenotype of STGD1 and LCA10 mouse models**

To determine whether the photoreceptor transduction obtained with AAV intein vectors could be therapeutically relevant, we tested them in the retina of STGD1 and LCA10 mouse models (*Abca4*<sup>-/-</sup> and *rd16* mice). One-month-old *Abca4*<sup>-/-</sup> mice were injected subretinally with AAV2/8-GRK1-ABCA4 intein vectors (dose of each vector per eye,  $4.3 \times 10^9$  to  $4.8 \times 10^9$  GC). Three months later, we harvested the eyes and performed transmission electron microscopy analysis of retinal ultrathin sections to measure the amounts of lipofuscin, which accumulates in the RPE of *Abca4*<sup>-/-</sup> mice (26, 27).

We found that RPE lipofuscin accumulation was significantly reduced in the *Abca4*<sup>-/-</sup> eyes injected with AAV intein vectors but not in negative control-injected eyes ( $P = 0.0163$ ; Fig. 7A and fig. S22). Naïve uninjected *Abca4*<sup>-/-</sup> mice were not included because we have shown that subretinal injections per se induce lipofuscin granules (28); therefore, the appropriate controls for the effect of ABCA4 gene delivery on lipofuscin reduction are sham-injected *Abca4*<sup>-/-</sup> mice. In parallel, 4- to 6-day-old *rd16* mice were injected subretinally with AAV2/8-GRK1-CEP290 intein vectors (dose of each vector per eye,  $5.5 \times 10^8$  GC). Microscopy analysis of retinal sections 1 month after injection showed that the thickness of the ONL, which includes photoreceptor nuclei, was significantly reduced in *rd16* mice compared with wild-type mice ( $P = 0.00750$ ; Fig. 7B), as a result of progressive retinal degeneration (25). We found that the ONL thickness in the *rd16* retinas injected with AAV

Downloaded from https://www.science.org on February 11, 2024

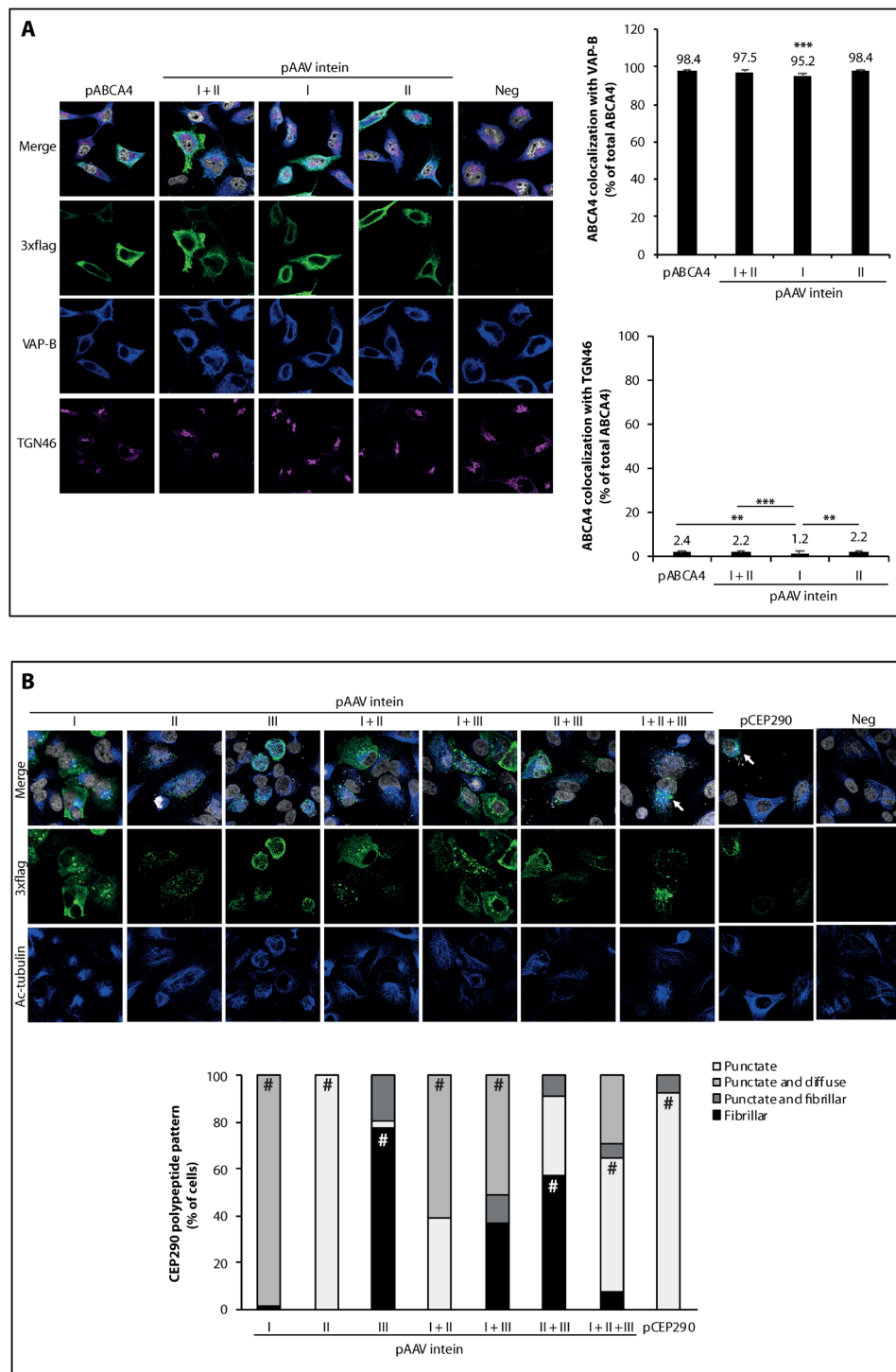


**Fig. 4. ABCA4 and CEP290 proteins from AAV intein vectors have a distribution pattern similar to those from full-length plasmids.** Representative images of immunofluorescence analysis of HeLa cells transfected with either AAV-shCMV-ABCA4 (A) or AAV-shCMV-CEP290 (B) intein plasmids. pABCA4 (A) or pCEP290 (B): plasmid including the full-length expression cassette; pAAV intein: AAV intein plasmids [either set 1 in (A) or set 5 in (B)]; I + II + III: AAV I + II + III intein plasmids; I + II: AAV I + II intein plasmids; I + III: AAV I + III intein plasmids; II + III: AAV II + III intein plasmids; I: single AAV I intein plasmid; II: single AAV II intein plasmid; III: single AAV III intein plasmid; Neg: untransfected cells. Cells were stained for 3xflag and either vesicle-associated membrane protein-associated protein B/C (VAP-B, ER marker) and TGN46 (trans-Golgi network marker) in (A) or acetylated tubulin (marker of microtubules) in (B). White arrows point at cells shown at higher magnification in fig. S16. Quantification of both ABCA4 colocalization with VAP-B and TGN46 markers (A) and cells showing the various CEP290 polypeptide patterns (B) are shown in the graphs. At least 150 cells for each condition were counted in  $n = 3$  independent experiments. (A) Significant differences between groups were assessed using Kruskal-Wallis test followed by pairwise comparisons using Wilcoxon rank sum test.  $**P < 0.01$  and  $***P < 0.001$ . Asterisks above the pAAV intein I column in the upper graph indicate significant differences with pABCA4, I + II, and II. (B) Significant differences between patterns of each column were assessed using binomial distribution. # indicates the predominant pattern for each CEP290 polypeptide ( $P < 0.00001$ ).

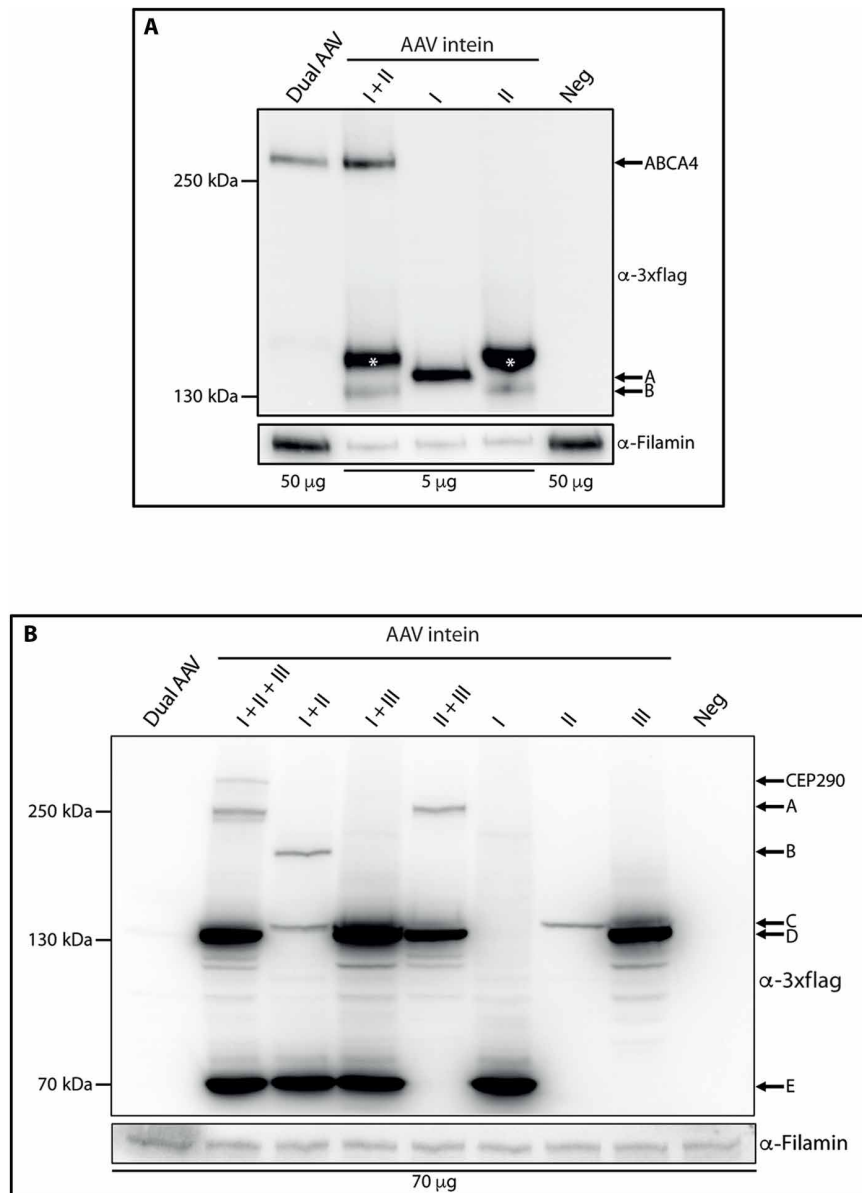


**Fig. 5. ABCA4 and CEP290 large protein reconstitution by AAV intein and dual AAV vectors.** WB analysis of lysates from HEK293 cells infected with either dual or intein AAV2/2-shCMV-ABCA4 (A) or AAV2/2-shCMV-CEP290 (B) vectors. AAV intein: AAV-ABCA4 [set 1; (A)] or AAV-CEP290 [set 5; (B)] intein vectors; I + II + III: AAV I + II + III intein vectors; I + II: AAV I + II intein vectors; I + III: AAV I + III intein vectors; II + III: AAV II + III intein vectors; I: single AAV I intein vector; II: single AAV II intein vector; III: single AAV III intein vector; dual AAV: dual AAV vectors; Neg: AAV-EGFP vectors. (A) The arrows indicate the full-length ABCA4 protein; A, protein product derived from AAV I; B, protein product derived from AAV II; \*, protein product with a potentially different posttranslational modification. (B) The arrows indicate the full-length CEP290 protein; A, protein product derived from AAV II + III; B, protein product derived from AAV I + II; C, protein product derived from AAV II; D, protein product derived from AAV III; and E, protein product derived from AAV I. The WBs are representative of  $n = 3$  independent experiments.

intein vectors was significantly higher (about 60%;  $P = 0.00562$ ) than that of negative control-injected *rd16* retinas (Fig. 7B). Accordingly, retinal function tests based on pupillary light responses showed a significant higher pupil constriction (about 20%;  $P = 0.0005939$ ) in *rd16* mice injected with AAV intein vectors than in negative control-injected *rd16* eyes (Fig. 7C).

We additionally investigated the safety of AAV intein vectors in the retina. To this aim, we injected subretinally wild-type C57BL/6J mice with either AAV2/8-GRK1-ABCA4 or AAV2/8-GRK1-CEP290 intein vectors (dose of each ABCA4 vector per eye,  $4.3 \times 10^9$  GC; dose of each CEP290 vector per eye,  $1.1 \times 10^9$  GC) and measured retinal electrical activity by Ganzfeld electroretinogram at 6 and 4.5 months after injection, respectively. In both studies, a- and b-wave amplitudes were similar between mouse eyes that were injected with AAV intein vectors and eyes injected with negative controls (fig. S23). In addition, the thickness of the ONL measured by optical coherence tomography was similar between AAV intein- and negative control-injected eyes (fig. S24).

## DISCUSSION

Great efforts have been directed to overcome the challenge of delivering large genes with AAV vectors. One of the systems with potential for clinical translation relies on the use of multiple AAV vectors (dual or triple) each carrying one part of a large transgene expression cassette that gets reconstituted upon coinfection by the multiple AAV and their genome tail-to-head concatemerization/recombination (29). The retina, being small and enclosed, favors coinfection by multiple AAV vectors, and dual and triple AAV have been successfully used to expand AAV transfer capacity in the retina (4, 7, 30, 31). However, transduction efficiency of multiple AAV is lower than that of single AAV (4, 7, 8) and may not be sufficient for specific applications (7). Here, we have investigated the reconstitution of large proteins in the retina via intein-mediated protein trans-splicing, a method widely used to purify/modify recombinant proteins (9, 10, 12).

In the context of gene therapy, intein-mediated protein trans-splicing has been used to reconstitute large therapeutic proteins like factor VIII in the liver (32, 33), dystrophin in muscles (34), or the L-type calcium channel in cardiomyocytes (35), however with limited efficacy. Here, we show that inteins reconstitute large proteins in the retina of small- and large-animal models and in human retinal organoids, and this improves the retinal phenotype of animal models of STGD1 and LCA10. This may be well favored by the small subretinal space, as it does with dual AAV vectors.

The amounts of AAV intein-mediated large protein reconstitution largely exceed those achieved via AAV genome recombination by dual AAV vectors, the gold standard for large protein reconstitution, both in vitro and in pig photoreceptors. In the large pig retina, we found that the amounts of the reconstituted EGFP protein were comparable to those achieved by single AAV vectors. This is similar to what was observed with dual AAV where the efficiency of multiple AAV transduction is higher in the pig than in



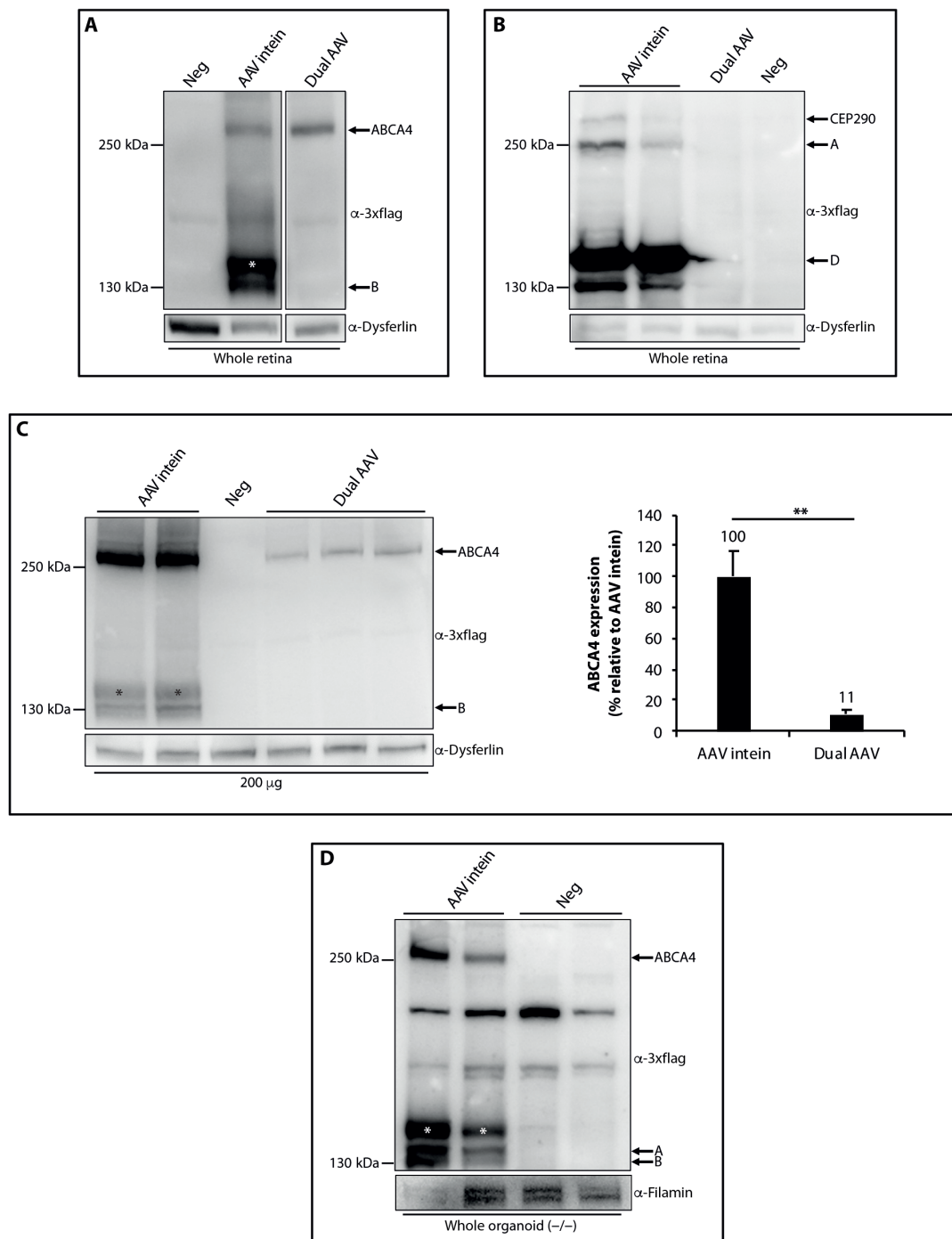


**Fig. 6. AAV intein vectors reconstitute large proteins in mouse, pig, and human photoreceptors.** (A and B) WB analysis of retinal lysates from either wild-type mice (A and B) or Large White pigs (C) injected with either dual or intein AAV2/8-GRK1-ABCA4 (A and C) or AAV2/8-GRK1-CEP290 (B) vectors. AAV intein, AAV intein vectors; Dual AAV, dual AAV vectors; Neg, either AAV-EGFP vectors or phosphate-buffered saline (PBS). Quantification of ABCA4 expression in Large White pigs injected with either dual ( $n = 3$ ) or intein ( $n = 2$ ) AAV2/8-GRK1-ABCA4 is included in (C). Significant differences between groups were assessed using unpaired Student's  $t$  test.  $^{***}P < 0.01$ . (D) WB analysis of lysates from human iPSC-derived 3D retinal organoids infected with AAV2/2-GRK1-ABCA4 intein vectors. AAV intein, AAV-ABCA4 intein vectors; Neg, not infected organoids;  $-/-$ , organoids derived from STGD1 patients. (A, C, and D) The arrows indicate the full-length ABCA4 protein (ABCA4); A, protein product derived from AAV I; B, protein product derived from AAV II; \*, protein product with a potentially different posttranslational modification. (B) The arrows indicate the full-length CEP290 protein (CEP290); A, protein product derived from AAV II + III; and D, protein product derived from AAV III. The WBs are representative of  $n = 11$  AAV intein- and 9 dual AAV-injected eyes (A);  $n = 10$  AAV intein- and 5 dual AAV-injected eyes (B); and  $n = 7$  AAV intein-infected organoids (D).

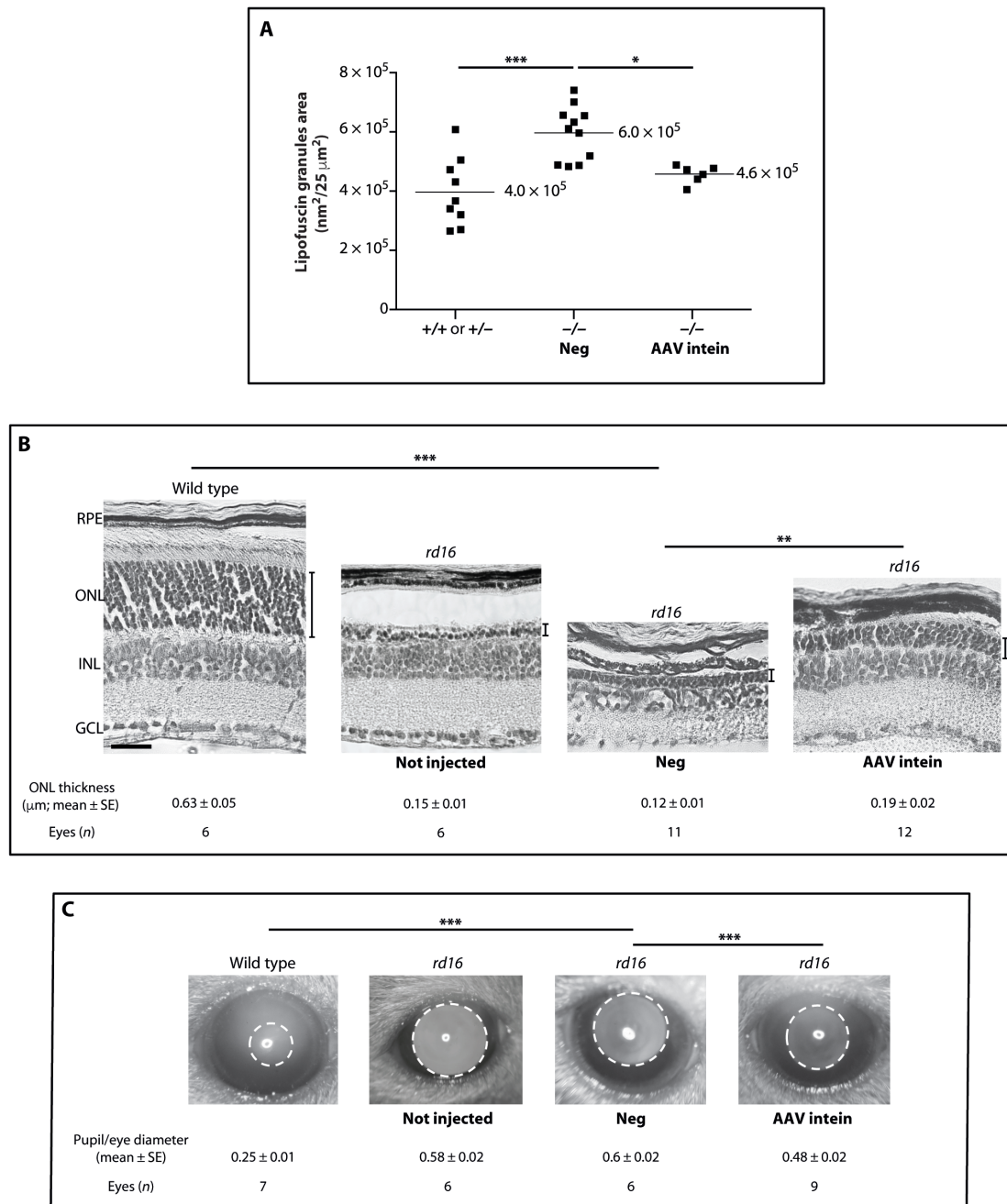


**Fig. 7. Subretinal administration of AAV intein improves the retinal phenotype of mouse models of inherited retinal degenerations.** (A) Quantification of the mean area occupied by lipofuscin in the RPE of *Abca4*<sup>-/-</sup> mice treated with AAV intein. Each filled square represents the mean value measured for each eye. The mean value of the lipofuscin area for each group is indicated in the graph. +/+ or +/-, control-injected *Abca4*<sup>+/+</sup> or *Abca4*<sup>+/-</sup> eyes (PBS); -/- Neg, negative control-injected *Abca4*<sup>-/-</sup> eyes (AAV I ABCA4, AAV II ABCA4, or PBS); -/- AAV intein, *Abca4*<sup>-/-</sup> eyes injected with AAV intein vectors. Significant differences between groups were assessed using one-way ANOVA followed by Tukey multiple pairwise-comparison. \* $P < 0.05$  and \*\*\* $P < 0.001$ . (B) Representative images of retinal sections from wild-type uninjected and *rd16* mice either not injected or injected subretinally with AAV2/8-GRK1-CEP290 intein vectors (AAV intein) or with negative controls (Neg: AAV I + II, AAV II + III, or PBS). Scale bar, 25  $\mu\text{m}$ . The thickness of the ONL measured in each image is indicated by the vertical black line. INL, inner nuclear layer; GCL, ganglion cell layer. Significant differences between groups were assessed using Kruskal-Wallis test followed by pairwise comparisons using Wilcoxon rank sum test. \*\* $P < 0.01$  and \*\*\* $P < 0.001$ . (C) Representative images of eyes from wild-type uninjected and *rd16* mice either not injected or injected subretinally with AAV2/8-GRK1-CEP290 intein vectors (AAV intein) or with negative controls (Neg: AAV I + II, AAV II + III, or PBS). White circles define pupils. Significant differences between groups were assessed using one-way ANOVA followed by Tukey multiple pairwise comparison. \*\*\* $P < 0.001$ . The complete set of  $P$  values can be found in data file S1.

the mouse retina (4, 7) and bodes well for future translation of this approach to the clinic. We show that AAV intein-mediated protein trans-splicing occurs in photoreceptors across species up to human from iPSC-derived retinal organoids.

One of the limitations we noted when applying trans-splicing to large proteins was that construct design needs to take into account (i) preservation at the junction points of amino acid residues needed for efficient protein trans-splicing and (ii) splitting of the proteins outside of structural domains to avoid incorrect polypeptide folding. We generated several sets of AAV intein constructs both for ABCA4 and CEP290 and found that their efficiency varied in terms of amount of protein reconstitution. In some cases, one of the two protein halves was less stable than the other, which presumably affected the quantity of full-length proteins produced. In addition, in one case (when using AAV-ABCA4 intein set 3), we found a band higher than full length, indicating a larger product, which could be the result of incomplete trans-splicing. According to our experience, construct design is more critical for AAV intein than for dual AAV, where the use of exogenous recombinogenic sequences and splicing signals allows splitting of a large coding sequence independently of the native protein structure and organization.

In addition, when using intein-mediated protein trans-splicing, each polypeptide is expressed from an independent expression cassette that needs to carry the required transcriptional elements that will be included in each of the AAV intein vectors. This is different from dual AAV, where the single large expression cassette is split into two halves, with the promoter element present only in the 5' vector and the polyA signal in the 3' vector. Therefore, when using AAV intein vectors, one limitation is that part of the cloning capacity will be taken up by regulatory elements that need to be replicated within each vector. This might be limiting in terms of size constraint; thus, to accommodate in two AAV intein vectors the coding sequence of large proteins, such as CEP290, short regulatory elements are required. However, these shorter elements are often weak in terms of transcriptional activity. Here, we show that splitting CEP290 into three polypeptides rather than two allows to accommodate into each AAV vector larger or more potent regulatory elements (full-length promoters or WPRE), and this leads to more efficient full-length protein expression than that obtained with two AAV intein vectors with weaker regulatory elements despite the need to achieve coinfection of the same cell by three vectors. Pivotal to the development of triple AAV intein vectors has been the use of different inteins, mDnaE/DnaE and DnaB, which do not cross-react, thus preventing improper trans-splicing between the polypeptides produced by AAV I and AAV III.

Despite this extensive optimization, the amounts of therapeutic large proteins we achieved by intein-mediated protein trans-splicing tend to be lower than those achieved for EGFP compared with a full-length expression cassette, suggesting that large therapeutic proteins appear to be more challenging to reconstitute than the small and stable EGFP. However, the amount of AAV intein ABCA4 in whole retinal lysates was about 10% of the endogenous protein. This expression is the result of only one third of the retina exposed to AAV.

For efficient trans-splicing to occur, the different polypeptide fragments should reside in the same subcellular compartment. This might be particularly critical for trans-membrane proteins like ABCA4, in which the two halves might be targeted to different compartments. Our immunofluorescence analysis shows that both the N- and C-terminal halves of ABCA4 localize to the ER *in vitro*, suggesting that trans-splicing might occur early after translation, thus assuring proper further targeting of the full-length protein. Proper protein

assembly is also confirmed by protein sequencing of trans-spliced ABCA4, as well as by the presence of the correctly excised split intein after trans-splicing. The improvement in the retinal phenotype of the two STGD1 and LCA10 animal models of inherited retinal diseases after subretinal injection of the AAV intein vectors strongly suggests that the reconstituted proteins have been properly processed and were functional.

An additional limitation of the AAV intein platform is the presence of both intein excised from the mature protein and truncated protein products that derive from either non-trans-spliced polypeptides or trans-splicing occurring only between two of three polypeptides (for CEP290 protein). Although these additional protein products are in some instances more abundant than the full-length proteins, they do not appear to be toxic. Strategies aiming at maximizing the equimolar amount of single polypeptides in target cells (for instance, by modulating their doses based on their different stability, for example, by increasing the dose of the AAV intein vector expressing the less stable polypeptide) could result in optimal trans-splicing and could lower the quantity of the more stable single polypeptide.

Similarly, excised inteins are produced upon trans-splicing. A method to reduce them can be envisaged, which is based on the inclusion between the two split inteins of a sequence, which mediates their selective degradation after splicing, as we have previously successfully done with dual AAV vectors (28). Regardless, our *in vivo* electrophysiological and morphological analyses show no signs of toxicity up to 4.5 and 6 months after injection in eyes injected with either AAV-CEP290 or AAV-ABCA4 intein vectors, respectively, although definitive assessment of the safety of AAV intein will require formal long-term toxicity studies.

In conclusion, we have shown that AAV intein-mediated protein trans-splicing reconstitutes large proteins both *in vitro* and in the mouse and pig retina and in human retinal organoids. Whereas some proteins can be efficiently reconstituted with two AAV intein vectors, others that are larger and require the use of large robust regulatory elements require three AAV intein vectors. Thus, careful design and optimization of the AAV intein constructs are required to achieve efficient protein trans-splicing. Subretinal administration of AAV intein vectors resulted in improvement of the retinal phenotype of STGD1 and LCA10 mouse models, thus providing evidence of the therapeutic potential of AAV intein vectors for gene therapy of these and other blinding diseases due to mutations in large genes.

## MATERIALS AND METHODS

### Study design

This study was designed to define the efficiency of AAV intein-mediated protein trans-splicing in reconstituting large proteins in the retina. This was defined by comparing the efficiency of protein expression achieved via protein trans-splicing to that achieved using reference platforms (normal size and dual AAV vectors) and by evaluating the impact of subretinal delivery of AAV intein on the retinal phenotype of animal models of inherited retinal diseases. In all *in vivo* studies, right and left eyes were randomly assigned to each treatment group. In addition, in the studies on the disease models, female and male mice were considered equivalent and randomly assigned to treatment groups. Littermate controls were used when available. Protein expression in the *in vitro* and *in vivo* studies was quantified objectively using the ImageJ software (for WB analysis) or a spectrophotometer to measure the optical density at 450 nm (for

ELISA analysis), without blinding. The experimenters in the efficacy and toxicity studies were blind to both genotype and treatment of the animals. Sample sizes were determined on the basis of previous experience and technical feasibility; at least three biological replicates in culture experiments or five animals per group were used in all the experiments, as indicated in the Results section and figure legends.

### Statistical analysis

Data are presented as means ( $\pm$ SE), which have been calculated using the number of independent *in vitro* experiments or eyes (not replicate measurements of the same sample). Statistical *P* values  $\leq 0.05$  were considered significant. The normality assumption was verified using the Shapiro-Wilk test. Data were analyzed by either the Student's *t* test or one-way ANOVA. Kruskal-Wallis rank sum test (nonparametric test) was used when ANOVA assumptions were not met. Pairwise comparisons between group levels with corrections for multiple testing were performed to determine whether the mean difference between specific pairs of groups is statistically significant.

In experiments where internal reference samples were used to normalize data across different replicates, their expression was set to either 100% or 1, as indicated in each graph. To show the internal variability of these internal reference samples, we calculated their expression as percentage relative to selected samples, as described in the following: fig. S2: pEGFP versus pAAV I + II,  $138.7 \pm 17.4$ ; fig. S4: EGFP versus DnaE,  $5.01 \pm 0.14$ ; fig. S8: EGFP versus DnaE,  $0.38 \pm 0.13$ ; fig. S10: EGFP versus DnaE,  $0.60 \pm 0.19$ ; fig. S12: EGFP versus DnaE,  $6.2 \pm 0.35$ ; Fig. 3A: set 1 versus set 2,  $274.2 \pm 46.5$ ; Fig. 3B: set 5 versus set 1,  $529.4 \pm 69.4$ ; fig. S17A: pABCA4 versus set 1,  $213.9 \pm 51.5$ ; and fig. S17B: pCEP290 versus set 5,  $238.6 \pm 38.2$ . Original data including specific statistical values are provided in data file S1.

### SUPPLEMENTARY MATERIALS

stm.sciencemag.org/cgi/content/full/11/492/eaav4523/DC1

Materials and Methods

Fig. S1. EGFP fluorescence in HEK293 cells transfected with AAV I + II but not single AAV I or AAV II intein plasmids.

Fig. S2. Similar EGFP expression after transfection of either AAV intein or single plasmids.

Fig. S3. *In vitro* EGFP expression from single, dual, and AAV intein vectors.

Fig. S4. Intein relative to full-length protein in HEK293 cells.

Fig. S5. AAV intein vectors reconstitute EGFP in both mouse RPE and photoreceptors.

Fig. S6. EGFP fluorescence from photoreceptor cells in mouse retinas injected with single, dual, and AAV intein vectors.

Fig. S7. EGFP expression from single, dual, and AAV intein vectors in mouse photoreceptors.

Fig. S8. Intein relative to full-length EGFP in mouse photoreceptors.

Fig. S9. EGFP expression from single, dual, and AAV intein vectors in pig photoreceptors.

Fig. S10. Intein relative to full-length protein in pig photoreceptors.

Fig. S11. Characterization and AAV intein-mediated transduction of human iPSC-derived 3D retinal organoids.

Fig. S12. Intein relative to full-length EGFP in human 3D retinal organoids.

Fig. S13. Schematic representation of the various sets of AAV-ABCA4 and AAV-CEP290 intein.

Fig. S14. Combination of heterologous N- and C-inteins does not result in detectable EGFP protein reconstitution *in vitro*.

Fig. S15. The amino acid sequence of ABCA4 reconstituted by AAV intein matches that of wild-type ABCA4.

Fig. S16. CEP290 aligns along microtubules.

Fig. S17. ABCA4 and CEP290 expression after transfection of either AAV intein or single plasmids.

Fig. S18. Subretinal delivery of AAV intein vectors results in ABCA4 expression in the mouse retina.

Fig. S19. Subretinal delivery of AAV intein vectors results in CEP290 expression in the mouse retina.

Fig. S20. AAV intein vectors reconstitute about 10% of endogenous Abca4.

Fig. S21. AAV intein vectors reconstitute full-length ABCA4 protein in human retinal organoids.

Fig. S22. Subretinal administration of AAV intein vectors results in reduction of lipofuscin accumulation in *Abca4*<sup>-/-</sup> mice.

Fig. S23. Subretinal delivery of AAV intein vectors in mice does not modify retinal electrical activity.

Fig. S24. Subretinal delivery of AAV intein vectors in mice does not modify the ONL thickness.

Data file S1. Raw data (provided as a separate Excel file).

Data file S2. Auxiliary images (provided as a separate PDF file).

Data file S3. EGFP peptide (provided as a separate Excel file).

### REFERENCES AND NOTES

1. FDA approves hereditary blindness gene therapy. *Nat. Biotechnol.* **36**, 6 (2018).
2. I. Trapani, A. Auricchio, Seeing the light after 25 years of retinal gene therapy. *Trends Mol. Med.* **24**, 669–681 (2018).
3. A. Auricchio, A. J. Smith, R. R. Ali, The future looks brighter after 25 years of retinal gene therapy. *Hum. Gene Ther.* **28**, 982–987 (2017).
4. I. Trapani, P. Colella, A. Sommella, C. Iodice, G. Cesi, S. de Simone, E. Marrocco, S. Rossi, M. Giunti, A. Palfi, G. J. Farrar, R. Polishchuk, A. Auricchio, Effective delivery of large genes to the retina by dual AAV vectors. *EMBO Mol. Med.* **6**, 194–211 (2014).
5. D. Duan, Y. Yue, J. F. Engelhardt, Expanding AAV packaging capacity with trans-splicing or overlapping vectors: A quantitative comparison. *Mol. Ther.* **4**, 383–391 (2001).
6. Z. Yan, Y. Zhang, D. Duan, J. F. Engelhardt, Trans-splicing vectors expand the utility of adeno-associated virus for gene therapy. *Proc. Natl. Acad. Sci. U.S.A.* **97**, 6716–6721 (2000).
7. A. Maddalena, P. Tornabene, P. Tiberi, R. Minopoli, A. Manfredi, M. Mutarelli, S. Rossi, F. Simonelli, J. K. Naggert, D. Cacchiarelli, A. Auricchio, Triple vectors expand AAV transfer capacity in the retina. *Mol. Ther.* **26**, 524–541 (2018).
8. P. Colella, I. Trapani, G. Cesi, A. Sommella, A. Manfredi, A. Puppo, C. Iodice, S. Rossi, F. Simonelli, M. Giunti, M. L. Bacci, A. Auricchio, Efficient gene delivery to the cone-enriched pig retina by dual AAV vectors. *Gene Ther.* **21**, 450–456 (2014).
9. O. Novikova, N. Topilina, M. Belfort, Enigmatic distribution, evolution, and function of inteins. *J. Biol. Chem.* **289**, 14490–14497 (2014).
10. K. V. Mills, M. A. Johnson, F. B. Perler, Protein splicing: How inteins escape from precursor proteins. *J. Biol. Chem.* **289**, 14498–14505 (2014).
11. N. H. Shah, E. Eryilmaz, D. Cowburn, T. W. Muir, Extein residues play an intimate role in the rate-limiting step of protein trans-splicing. *J. Am. Chem. Soc.* **135**, 5839–5847 (2013).
12. Y. Li, Split-inteins and their bioapplications. *Biotechnol. Lett.* **37**, 2121–2137 (2015).
13. N. H. Shah, T. W. Muir, Inteins: Nature's gift to protein chemists. *Chem. Sci.* **5**, 446–461 (2014).
14. C. Schmela, D. Grimm, Split Cas9, no hairs—Advancing the therapeutic index of CRISPR technology. *Biotechnol. J.* **13**, e1700432 (2018).
15. L. Villiger, H. M. Grisch-Chan, H. Lindsay, F. Ringhald, C. B. Pogliano, G. Allegri, R. Fingerhut, J. Häberle, J. Matos, M. D. Robinson, B. Thöny, G. Schwank, Treatment of a metabolic liver disease by *in vivo* genome base editing in adult mice. *Nat. Med.* **24**, 1519–1525 (2018).
16. H. Iwai, S. Züger, J. Jin, P. H. Tam, Highly efficient protein trans-splicing by a naturally split DnaE intein from *Nostoc punctiforme*. *FEBS Lett.* **580**, 1853–1858 (2006).
17. J. Zettler, V. Schütz, H. D. Mootz, The naturally split Npu DnaE intein exhibits an extraordinarily high rate in the protein trans-splicing reaction. *FEBS Lett.* **583**, 909–914 (2009).
18. C. Mussolino, M. della Corte, S. Rossi, F. Viola, U. di Vicino, E. Marrocco, S. Neglia, M. Doria, F. Testa, R. Giovannoni, M. Crasta, M. Giunti, E. Villani, M. Lavitrano, M. L. Bacci, R. Ratiglia, F. Simonelli, A. Auricchio, E. M. Surace, AAV-mediated photoreceptor transduction of the pig cone-enriched retina. *Gene Ther.* **18**, 637–645 (2011).
19. T. Nakano, S. Ando, N. Takata, M. Kawada, K. Muguruma, K. Sekiguchi, K. Saito, S. Yonemura, M. Eiraku, Y. Sasai, Self-formation of optic cups and storable stratified neural retina from human ESCs. *Cell Stem Cell* **10**, 771–785 (2012).
20. X. Zhong, C. Gutierrez, T. Xue, C. Hampton, M. N. Vergara, L. H. Cao, A. Peters, T. S. Park, E. T. Zambidis, J. S. Meyer, D. M. Gamm, K. W. Yau, M. V. Canto-Soler, Generation of three-dimensional retinal tissue with functional photoreceptors from human iPSCs. *Nat. Commun.* **5**, 4047 (2014).
21. M. Cheriyan, S. H. Chan, F. Perler, Traceless splicing enabled by substrate-induced activation of the *Nostoc punctiforme* Npu DnaE intein after mutation of a catalytic cysteine to serine. *J. Mol. Biol.* **426**, 4018–4029 (2014).
22. J. E. Donello, J. E. Loeb, T. J. Hope, Woodchuck hepatitis virus contains a tripartite posttranscriptional regulatory element. *J. Virol.* **72**, 5085–5092 (1998).
23. N. Zhang, Y. Tsybovsky, A. V. Kolesnikov, M. Rozanowska, M. Swider, S. B. Schwartz, E. M. Stone, G. Palczewska, A. Maeda, V. J. Kefalov, S. G. Jacobson, A. V. Cideciyan, K. Palczewski, Protein misfolding and the pathogenesis of ABCA4-associated retinal degenerations. *Hum. Mol. Genet.* **24**, 3220–3237 (2015).
24. H. Sun, P. M. Smallwood, J. Nathans, Biochemical defects in ABCR protein variants associated with human retinopathies. *Nat. Genet.* **26**, 242–246 (2000).
25. T. G. Drivas, E. L. Holzbaur, J. Bennett, Disruption of CEP290 microtubule/membrane-binding domains causes retinal degeneration. *J. Clin. Invest.* **123**, 4525–4539 (2013).
26. N. L. Mata, R. T. Tzekov, X. Liu, J. Weng, D. G. Birch, G. H. Travis, Delayed dark-adaptation and lipofuscin accumulation in *abcr*<sup>+/-</sup> mice: Implications for involvement of ABCR in age-related macular degeneration. *Invest. Ophthalmol. Vis. Sci.* **42**, 1685–1690 (2001).
27. J. Weng, N. L. Mata, S. M. Azarian, R. T. Tzekov, D. G. Birch, G. H. Travis, Insights into the function of Rim protein in photoreceptors and etiology of Stargardt's disease from the phenotype in *abcr* knockout mice. *Cell* **98**, 13–23 (1999).

28. I. Trapani, E. Toriello, S. de Simone, P. Colella, C. Iodice, E. V. Polishchuk, A. Sommella, L. Colecchi, S. Rossi, F. Simonelli, M. Giunti, M. L. Bacci, R. S. Polishchuk, A. Auricchio, Improved dual AAV vectors with reduced expression of truncated proteins are safe and effective in the retina of a mouse model of Stargardt disease. *Hum. Mol. Genet.* **24**, 6811–6825 (2015).
29. M. E. McClements, R. E. MacLaren, Adeno-associated virus (AAV) dual vector strategies for gene therapy encoding large transgenes. *Yale J. Biol. Med.* **90**, 611–623 (2017).
30. F. M. Dyka, S. L. Boye, V. A. Chiodo, W. W. Hauswirth, S. E. Boye, Dual adeno-associated virus vectors result in efficient in vitro and in vivo expression of an oversized gene, MYO7A. *Hum. Gene Ther. Methods* **25**, 166–177 (2014).
31. V. S. Lopes, S. E. Boye, C. M. Louie, S. Boye, F. Dyka, V. Chiodo, H. Fofa, W. W. Hauswirth, D. S. Williams, Retinal gene therapy with a large MYO7A cDNA using adeno-associated virus. *Gene Ther.* **20**, 824–833 (2013).
32. F. Zhu, Z. Liu, X. Chi, H. Qu, Protein trans-splicing based dual-vector delivery of the coagulation factor VIII gene. *Sci. China Life Sci.* **53**, 683–689 (2010).
33. F. Zhu, Z. L. Liu, X. L. Wang, J. Miao, H. G. Qu, X. Y. Chi, Inter-chain disulfide bond improved protein trans-splicing increases plasma coagulation activity in C57BL/6 mice following portal vein FVIII gene delivery by dual vectors. *Sci. China Life Sci.* **56**, 262–267 (2013).
34. J. Li, W. Sun, B. Wang, X. Xiao, X. Q. Liu, Protein trans-splicing as a means for viral vector-mediated in vivo gene therapy. *Hum. Gene Ther.* **19**, 958–964 (2008).
35. P. Subramanyam, D. D. Chang, K. Fang, W. Xie, A. R. Marks, H. M. Colecraft, Manipulating L-type calcium channels in cardiomyocytes using split-intein protein transsplicing. *Proc. Natl. Acad. Sci. U.S.A.* **110**, 15461–15466 (2013).

**Acknowledgments:** We thank the following people from TIGEM, Naples, Italy: A. Carissimo (Bioinformatics Core) for the statistical analysis, the AAV Vector Core for AAV vector production, E. Nusco for help with mice injections, the Microscopy Core for assistance in microscope imaging, and G. Diez-Roux (Scientific Office) and N. Brunetti-Pierri for the critical reading of the manuscript. **Funding:** This work was supported by the European Research

Council (ERC) (grant number 694323 “EYEGET” to A.A.), the Telethon Foundation (grant number TGM16MT1 to A.A.), and the University of Naples Federico II under the STAR Program (to I.T.). M.A.D.M. acknowledges the support of Telethon Foundation (grant number TGM11CB1), Associazione Italiana per la Ricerca sul Cancro (grant number IG2013\_14761), and ERC (Advanced Investigator grant number 670881 “SYSMET”). **Author contributions:** The study was conceived, designed, and written by A.A., P. Tornabene, and I.T. All data were generated by P. Tornabene and I.T. with the technical help of R.M., M.C., M.L., and S.d.S.P. Tornabene developed retinal organoids and performed the in vitro and in vivo experiments of EGFP and CEP290. I.T. performed the in vitro and in vivo experiments of ABCA4. F.D.A. and E.M. performed the morphological and functional analyses in vivo. A.I. performed statistical analysis. P. Tiberi, C.I., C.G., S.R., E.M.S., and F.S. performed injections in mice and pigs. L.G. and M.A.D.M. performed studies on ABCA4 localization in cells. S.A., C.B.H., and F.P.M.C. provided iPSC cell lines. E.P. and R.P. supervised and performed electron microscopy analysis. **Competing interests:** A.A., P. Tornabene, and I.T. are coinventors on patent application number EP 18200490.3 entitled “Intein proteins and uses thereof.” The other authors declare that they have no competing interests. **Data and materials availability:** All data associated with this study are present in the paper or the Supplementary Materials.

Submitted 17 September 2018  
Resubmitted 21 November 2018  
Accepted 4 April 2019  
Published 15 May 2019  
10.1126/scitranslmed.aav4523

**Citation:** P. Tornabene, I. Trapani, R. Minopoli, M. Centrolo, M. Lupo, S. de Simone, P. Tiberi, F. Dell’Aquila, E. Marrocco, C. Iodice, A. Iuliano, C. Gesualdo, S. Rossi, L. Giaquinto, S. Albert, C. B. Hoyng, E. Polishchuk, F. P. M. Cremers, E. M. Surace, F. Simonelli, M. A. De Matteis, R. Polishchuk, A. Auricchio, Intein-mediated protein trans-splicing expands adeno-associated virus transfer capacity in the retina. *Sci. Transl. Med.* **11**, eaav4523 (2019).